Journal of Renewable Energy and Sustainable Development (RESD) Volume 11, Issue 1, June 2025 - ISSN 2356-8569
http://dx.doi.org/10.21622/RESD.2025.11.1.1264
Received on, 21 March 2025 Accepted on, 18 May 2025 Published on, 25 May 2025

Intelligent Hybrid Method to Predict Generated Power of Solar PV System

Prashant Singh [1*], Navneet Kumar Singh [2], and Asheesh Kumar Singh [3]

[1,2,3] Motilal Nehru National Institute of Technology Allahabad, Department of Electrical Engineering, Prayagraj, Uttar Pradesh, India

prashantsingh@mnnit.ac.in, navneet@mnnit.ac.in, asheesh@mnnit.ac.in

ABSTRACT

This paper presents a short-term hybrid solar photovoltaic (PV) power forecasting model called empirical mode decomposition (EMD)-particle swarm optimization (PSO)-adaptive neuro-fuzzy inference system (ANFIS), i.e., refer to EPA. The model offers a solution to the challenge of accurately predicting generated solar PV power while considering the dynamic nature of environmental variables and solar radiation variability. In the first stage, EMD is applied to decompose the raw solar power series signal into a finite set of IMFs and a residue to enhance forecasting accuracy. The broken-input solar PV power data is fed into the ANFIS, along with meteorological variables. In the second stage, the characteristics of the individual component signals are modeled and forecasted separately using ANFIS with different membership functions. They are then compared to select the best input membership function, i.e., Gaussian. The swarm optimization is used to optimize the parameters of the EMD-ANFIS for enhanced accuracy. Utilizing empirical mode reconstruction of the optimized output, the predicted power of the solar PV system is computed. The suggested hybrid model's performance is evaluated and compared to alternative forecasting methods. It is discovered that the suggested model produces more accurate forecasts in terms of nMAE = 0.1870, nRMSE = 0.2723, and nMSE = 34.71. Additionally, the proposed model demonstrates robustness across various weather conditions, highlighting its applicability and effectiveness. Overall, this paper aims to explain the benefits of using a hybrid model instead of a standalone one, thereby enhancing the reliability and efficiency of solar PV power forecasting systems.

Index-words: *Adaptive neuro-fuzzy inference system (ANFIS), Empirical Mode Decomposition (EMD), Forecasting, Particle swarm optimization (PSO), Photovoltaic, and Solar power.*

I. INTRODUCTION

Today, electricity plays a crucial role in our daily lives, powering our homes, businesses, and industries. However, as the global population continues to increase, the demand for energy resources has surged, placing unprecedented pressure on our planet's finite fossil fuel reserves. This escalating demand has led to a critical need for exploring alternative sources of energy that are both sustainable and environmentally friendly. Among these alternatives, solar photovoltaic (PV) power generation has emerged as a promising solution. Solar PV systems offer a renewable and clean electricity source by harnessing the abundant energy from the sun. Unlike fossil fuels, which emit harmful greenhouse gases when burnt for energy, solar power generation produces minimal emissions, mitigating the adverse effects of climate change [1], [2]. At the same time, the factors that influence energy consumption and power generation must also be considered. Electric load forecasting is vital in power system planning and electricity scheduling. Long-term forecasting (one month to one year), medium-term forecasting (one week to one month), and short-term forecasting (one hour to twenty-four hours) are all included [3], [4].

Artificial Neural Networks (ANN) have emerged as a significant departure from linear algorithms towards non-linear solutions. ANN modeling has outperformed conventional mathematical models in terms of accuracy and adaptability [5]. These models also show the problem of overlearning and their reliability in forecasting, which can be compromised by the randomness of initial datasets [6]. In response to these challenges, some authors have suggested adaptive neuro-fuzzy inference systems [7-9]. In [10], a prediction model for solar radiation was proposed, utilizing a predictive framework rooted in Recurrent Neural Networks (RNNs). This model combines Particle Swarm Optimization (PSO) and Evolutionary Algorithm (EA) techniques. Zhang et al. introduce a novel approach termed Genetic Algorithm-

cc BY NC
Copyright © 2025, authors

based Wavelet Neural Network (GA-WNN) for forecasting the power output of photovoltaic plants. This method enhances prediction accuracy by integrating conventional backpropagation and wavelet neural network techniques with genetic algorithms [11]. Cruz et al. introduce the application of regularisation techniques in a multiparametric linear regression model to predict the active power levels of a photovoltaic system. All prediction models had an accuracy greater than 99.97% with reduced training time [12]. In [13], the empirical mode decomposition-attention-long short-term memory model represents a promising approach for forecasting in energy markets. Its innovative architecture, combining empirical mode decomposition, attention mechanisms, and long short-term memory networks, enables it to achieve superior empirical performance compared to other advanced forecasting models. Perveen et al. [14] designed an ANFIS-based model for short-term power forecasting in smart grid contexts using data from a composite climate zone. Comparative analysis showed that ANFIS outperformed other models, including ANN, support vector machines, and fuzzy logic systems. Patel et al. [15] analyzed various ANN models and hybrid approaches combining ANN with fuzzy logic for predicting solar irradiation and PV generation. Their findings concluded that hybrid ANN–fuzzy models offer better predictive performance across different inputs and network structures. Viswavandya et al. [16] developed fuzzy logic and ANFIS models using historical weather data to forecast short-term solar irradiation and validated their accuracy against on-site radiation measurements, yielding promising outcomes.

Ndiaye [17] applied both a standard ANFIS model and an optimized ANFIS-GA variant to forecast PV power output for integration into Senegal's national grid. The ANFIS-GA model proved more effective, achieving a lower mean square error of 2.027 versus 4.142 from the basic ANFIS model. Khosravi et al. [18] developed ANFIS and ANN models optimized using both GA and PSO to simulate the thermal and energy performance of a Stirling solar collector, incorporating diverse meteorological inputs and design parameters. Among all models, PSO-optimised ANFIS delivered the most accurate results. Didem [19] analyzed industrial energy demand in Turkey using multiple linear regression, ANFIS, and PSO-ANFIS models. The results showed that PSO-ANFIS outperformed the others, offering the highest prediction accuracy and minimal estimation error. In the realm of solar energy research, several knowledge-based engineering methodologies, including the Artificial Intelligence, Adaptive Neuro-Fuzzy Inference System (ANFIS) [20], Artificial Neural Networks with the Fuzzy System (ANN-FS) [21], (PSO-NN) [22], Wavelet-ANFIS-PSO [23], EMD-ANN [24], [25], PSO-ANN [26], and AI classification models [27], have been applied extensively in recent years to facilitate comprehensive real-time forecasting and approximation investigations, contributing valuable insights to the field.

This study presents a hybrid short-term forecasting model, EMD–PSO–ANFIS (EPA), which combines Empirical Mode Decomposition and Particle Swarm Optimization to accurately predict solar PV power using historical data and effectively handle its nonlinear and variable nature. In the first phase of the model, EMD is employed to decompose the raw solar PV power time series into a set of Intrinsic Mode Functions (IMFs) and a residual component. This decomposition helps to split distinct signal patterns, making each component more stable and predictable and, thus, more suitable for accurate modeling. In the second phase, the decomposed IMFs and residuals are individually modeled and forecasted using Adaptive Neuro-Fuzzy Inference Systems (ANFIS). ANFIS is a powerful modeling tool capable of capturing complex and nonlinear relationships between input and output variables with high precision. Previous research has demonstrated the superior performance of ANFIS compared to both conventional and other AI-based forecasting methods [28]. To further enhance performance, the structure of each ANFIS model is optimized using the PSO algorithm. PSO is particularly well-suited for this task due to its simplicity, computational efficiency, and effectiveness in parameter optimization. By optimizing each component model separately, the EPA approach ensures that each IMF and the residual are accurately modeled. The final forecast is obtained by aggregating the forecasts of all individual components, thereby reconstructing the original time series with improved precision. Because the original solar PV power signal is inherently the sum of its IMFs and residual, this decomposition-based modeling approach maintains completeness while offering improved forecasting accuracy. The effectiveness of the proposed EPA model has been validated through comparative analysis with other forecasting methods, including standalone ANN, standalone ANFIS, and EMD–ANFIS without PSO optimization. Overall, the

http://dx.doi.org/10.21622/RESD.2025.11.1.1264

proposed EPA method leverages the simplicity and efficiency of PSO to optimize the complex ANFIS models, leading to a more robust and accurate solar PV power forecasting solution.

The main contributions of the work are as follows:

1. Development of a new hybrid forecasting model (EPA), which integrates signal decomposition, intelligent learning, and optimization techniques to accurately predict short-term solar PV power using historical generation data.

2. Application of Empirical Mode Decomposition (EMD) to isolate meaningful signal components (IMFs and residue) from raw solar PV power data, improving the stability and predictability of input features for enhanced model training.

3. Investigate the robustness of the optimal model by comparing overall prediction performances of standalone ANN, ANFIS and EMD–ANFIS, as well as examine the impact of the level of decomposition and types of input membership function under various performance evaluation metrics.

4. Compare the proposed EPA model with other standalone and hybrid models.

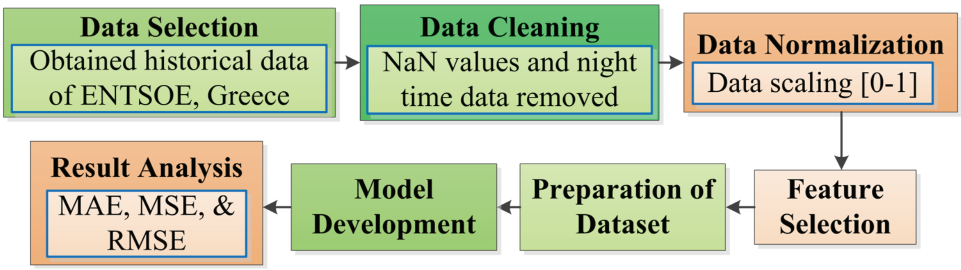

Fig.1. Process flow of the proposed model

The structure of this paper is as follows. The theoretical insights into the methodology of forecasting models and data pre-processing are explained in Section 2. The suggested hybrid forecasting models, including EPA model, are presented in Section 3. The results and conclusions are covered in Sections 4 and 5, respectively.

II. THEORETICAL BACKGROUND

This section has covered the theoretical foundations of data preprocessing and how to decompose solar PV data for forecasting models. The process flow of the EPA model is illustrated in Figure 1. Input variables include direct and diffuse radiation, temperature, and solar PV power. The process involves three key phases: data preprocessing, model development, and rule-base creation, followed by result analysis. A detailed explanation of the hybrid model construction is provided below and further elaborated in the next section:

A. Description of the Raw Dataset and Data Cleaning

The raw data used in this paper were sourced from the European Network of Transmission System Operators for Electricity, Greece (ENTSOE-G), Southeast Europe [29]. The dataset contains 24 entries per day of hourly records from January 1st, 2018, to December 31st, 2019. This dataset offers raw data for a total of 17,520 entries. The following table, i.e., Table I. gives the helpful data fields.

TABLE I. DETAILS OF DATASET

Feature	Unit
Solar PV power	MW
Temperature	Degree Celsius
Direct radiation	horizontal (Watt/m^2)
Diffuse radiation	horizontal (Watt/m^2)
Date	Duration (01/Jan/2018 – 31/Dec/2019)
Time	Selected hours (04:00 a.m. – 05:00 p.m.)

Data cleaning includes eliminating nighttime records from the solar PV data series. The data entries pertaining to the hours of 06:00 p.m. to 03:00 a.m. have been eliminated. It resulted in 10,220 entries from the original data being kept for further use. Preprocessed solar PV power data without normalization is depicted in Figure 2.

Volume 11, Issue 1, June 2025 - ISSN 2356-8569
http://dx.doi.org/10.21622/RESD.2025.11.1.1264

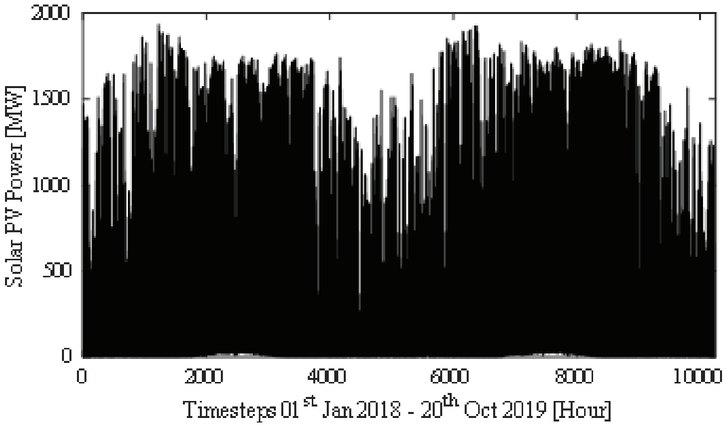

Fig. 2. Preprocessed solar PV power data (without night data points)

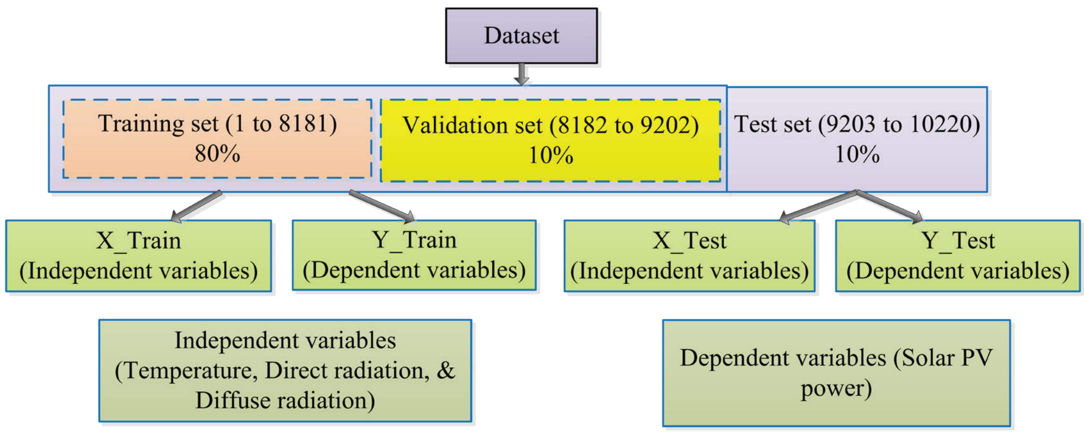

Fig. 3. Data split process

This data spans 10,220 samples, with a sample size of 40,880 data points (10,220 samples × 4 features). The data split process is demonstrated in Figure 3. The training set spans January 1st, 2018, to August 8th, 2019; the validation set covers August 8th, 2019, to October 20th, 2019; and the testing set includes data from October 20th, 2019, to December 31st, 2019.

B. *Process of Data Normalization Feature Selection*

Data normalization assigns the same weight to every input value, regardless of size. The values become uniform and dimensionless as a result. High-value variables may impact distance measurements more than other values, mainly when an algorithm employs Euclidean distance. This method reduces all values to a range of 0 to 1. These updated values originate [30-32] with:

$$\bar{K} = \frac{k - k_{\min}}{k_{\max} - k_{\min}} \tag{1}$$

Where k is the value being entered. The terms $k_{\min}$ k_{ii} denote the minimum and maximum values of the entered value, respectively. Once the data is normalized, relevant model-building and prediction features can be selected. This process involves identifying important input variables that will be factored into training the model and removing features that lack relevance or won't improve the model's accuracy. Doing so reduces the number of input variables, which reduces the time and complexity required to train the model. To enhance model performance, input variables with the most significant influence on the output are identified and retained. Historical values of meteorological inputs—ambient temperature, diffuse horizontal radiation, and direct horizontal radiation—are shifted backward by 1, 24, and 48 hours to construct a set of time-lagged predictor variables. The prediction model targets historical solar PV power output as the dependent variable. Based on correlation analysis, the most relevant input features selected are:

http://dx.doi.org/10.21622/RESD.2025.11.1.1264

- Solar PV power: $P_s(t-24) = 0.92$
- Temperature: $T(t-24) = 0.59$
- Direct radiation: $D_r(t-1) = 0.83$
- Diffuse radiation: $D_f(t-48) = 0.82$

Ultimately, the variables with the best correlations are then taken from each input. The variables $T(t-24)$, $D_f(t-48)$, $D_r(t-1)$, and $P_s(t-24)$ are selected as the preceding values for temperature, diffuse radiation, direct radiation, and solar PV power, respectively, based on the correlation analysis.

III. PROPOSED MODEL

A. Empirical Mode Decomposition

Huang et al. [33] introduced the Empirical Mode Decomposition (EMD) concept. It is widely utilized in signal processing applications for its ability to decompose complex signals into Intrinsic Mode Functions (IMFs), aiding in extracting meaningful oscillatory components. EMD uses a sifting process within each IMF iteratively, making EMD a data-driven technique that automatically extracts frequency components from a time series of data [34], [35]. The initial signal is split into several IMFs and a residue using the EMD. The underlying data can then be examined in greater detail by looking at each IMF component separately. EMD can be used to identify trends, frequencies, and periodicity to provide a better understanding of complex signals [36].

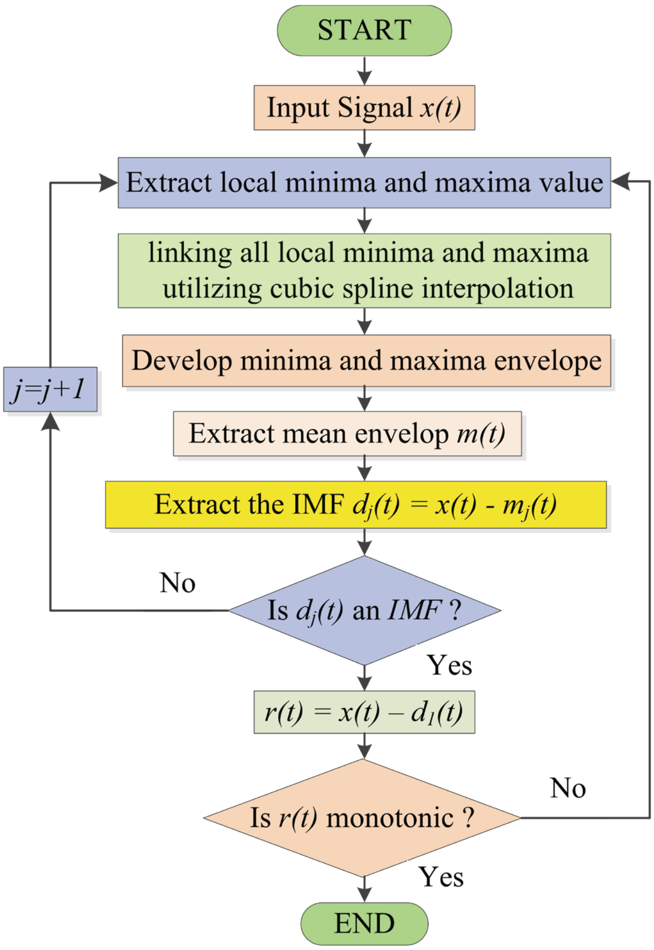

Fig. 4. EMD algorithm

Two essential features of the intrinsic mode function (IMF) are as follows:

1. An IMF's local maxima and minima counts do not deviate by more than 1.
2. The IMF waveform has an average value of zero.

As depicted in Figure 4., the EMD algorithm is implemented from start to end steps and step-by-step IMF extraction for EMD.

http://dx.doi.org/10.21622/RESD.2025.11.1.1264

Using the described approach to decompose the initial time series $x(t)$ into a set of IMFs signals $d_j(t)$ along with the residual component $r(t)$, written as follows:

$$x(t) = \sum_{j=1}^{\ddot{u}} d_j(t) + r(t) \tag{2}$$

$1 \le j \le$ number of IMF

Huang's formulation applied to generated solar PV power $P_s(t\text{-}24)$:

$$P_{\ddot{u}}(t-24) = \sum_{j=1}^{e} P^{\ddot{u}} {}^{j}(t-24) + P^{r_e}(t-24) \tag{3}$$

Where e is the total number of IMFs extracted and $P_s(t\text{-}24)$ is the solar PV power at time instance $(t\text{-}24)$.

For the first IMF extraction, the decomposed power component:

$$P_s^{IMF_1}(t-24) = P_s(t-24) - P_s^{r_1}(t-24) \tag{4}$$

Second IMF extraction:

$$P_s^{IMF_{\ddot{u}}}(t-24) = P_s^{r}(t-24) - P_s^{r}(t-24) \tag{5}$$

Third IMF extraction:

$$P_s^{IMF_3}(t-24) = P_s^{r_2}(t-24) - P_s^{r_3}(t-24) \tag{6}$$

Fourth IMF extraction:

$$P_s^{IMF_4}(t-24) = P_s^{r_3}(t-24) - P_s^{r_4}(t-24) \tag{7}$$

Final residual component after extracting 4th level of decomposition: $P_s^{r_4}(t-24)$ PSO-FIS predicts these decomposed components, which are then reconstructed using EMD to predict PV power.

B. Adaptive Neuro-Fuzzy Inference System

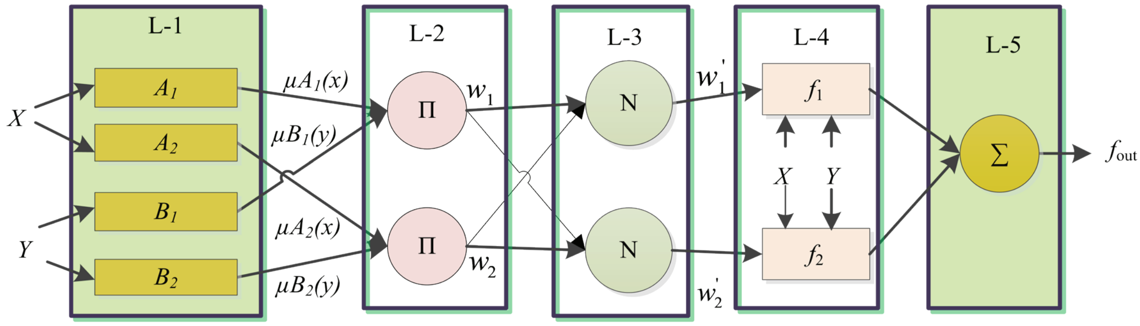

Fig. 5. Functional architecture of ANFIS network

Jang [37] introduced ANFIS in 1993 to address the challenges of non-linear systems. ANFIS utilizes fuzzy logic principles within an ANN framework to improve its cognitive capabilities. It combines fuzzy logic and neural networks based on the Takagi-Sugeno fuzzy inference system [38]. It uses fuzzy logic to structure a network of basic neurons, providing a more cognitively powerful combination. ANFIS eliminates the need for human experience and knowledge for parameter tuning [39], [40]. It integrates network learning and fuzzy logic processes [41]. In the network learning process, the inference parameters of a fuzzy system are tuned until they fit the training data. On the other hand, in the fuzzy logic process, the numerical inference mechanism is focused on the fuzzy knowledge base, the crisp if-then rules, and the output of the fuzzy set calculations.

The schematic representation of the ANFIS network is depicted in Figure 5. The adaptive network consists of five layers of nodes: the fuzzification layer, rule layer, normalization layer, defuzzification layer, and summation layer. Within the ANFIS system, premise and consequent parameters play a crucial role [42]. The fuzzification layer plays a significant role in allowing the system to identify patterns within the input data, which is made possible by the premise parameters. Conversely, consequent parameters {p, q, r} are linked with the membership functions of the defuzzification layer. The parameter was optimized using a training algorithm. In the proposed methodology, ANFIS system parameters are optimized using an EPA hybrid algorithm, which will be detailed further in subsequent sections.

L-1 (*Fuzzification layer*): The initial layer is depicted by squares, indicating its adjustable parameters. This layer receives and processes input to generate membership values ranging from 0 to 1. It calculates

 Volume 11, Issue 1, June 2025 - ISSN 2356-8569
http://dx.doi.org/10.21622/RESD.2025.11.1.1264

the membership values for each linguistic variable associated with a specified fuzzy variable. The resulting output is illustrated in (8) & (9).

$$O_{\ddot{u}}^{1} = \mu \quad (x) \tag{8}$$

$$O_{\ddot{u}}^{1} = \mu \quad (y) \tag{9}$$

for $i = 1, 2$

L-2 (*Rule layer*): Each node in this layer, represented by pie symbols, evaluates the firing strength of each rule by taking the product of the membership grade from L-1, as indicated by (10).

$$O_i^2 = \mu_{Ai}(x) * \mu_{Bi}(y) \tag{10}$$

for $i = 1, 2$

L-3 (*Normalisation layer*): The third layer normalizes the firing strengths computed in L-2 to obtain the normalized firing strengths. Mathematically, the normalized output of each node in L-3, as calculated by (11):

$$O_i^3 \aleph w_i' \quad \frac{w_i}{(\ddot{u}_1 + \quad _2)} \quad \frac{w_i}{\sum \quad _i} \tag{11}$$

for $i = 1, 2$

L-4 (*Defuzzification layer*): This layer computes the consequent parameters {p, q, r} based on the normalized firing strengths from L-3, as specified in (12).

$$O_i^{\ddot{u}} = w_i \times f_i = w_i \times (p_i x + q_i y + r_i) \tag{12}$$

for $i = 1, 2$

L-5 (*Summation layer*): Ultimately, the fifth layer combines the consequent parameters obtained from L-4 to generate the final output of the ANFIS system, as described in (13).

$$O_i^5 = f_{out} = \sum_i w_i' f_i \tag{13}$$

The parametric details of various ANFIS models: AGa (Gaussian MFs), AGb (G-bell MFs), and ATr (Trapezoidal MFs) are presented in Table II. This table shows that Gaussian, G-bell, and trapezoidal MFs are investigated using different antecedents and consequent parameters.

C. *The Proposed EPA Hybrid Method*

Hybridization of the PSO-tuned ANFIS model integrated with EMD-based data decomposition for precise PV power forecasting. EMD decomposes the generated solar PV power series into an intrinsic mode function (IMFs) with distinct frequency components, while a PSO-tuned ANFIS model with Gaussian input MFs predicts the future values of these IMFs. The forecasted solar PV power is obtained by applying the empirical mode reconstruction process to the predicted IMF components. This decomposition is particularly valuable given the complex frequency variations present in the generated solar PV power data, as described in the subsequent discussion.

Meteorological inputs, which vary significantly, impact solar photovoltaic power, introducing both high-frequency fluctuations and low-frequency patterns linked to Earth's rotation around the Sun. These combined components can degrade the forecasting accuracy. EMD efficiently separates these components into distinct time series, and the model reduces forecast error. EMD effectively identifies trends, frequencies, and periodicity to provide a better understanding of complex signals and improve overall forecasting performance.

In this work, solar power data is initially decomposed into intrinsic mode functions (*IMFs*) and a residual component (*r*) using EMD. A preliminary analysis, based on performance metrics, determines level 2 as the optimal decomposition level before conducting model-based comparisons. Level-2 EMD combined with a gaussian type input MF for ANFIS model performs well, leading to its selection for further model development.

TABLE II. PARAMETERS IN THE ANFIS MODEL WITH DIFFERENT INPUTS MFs

ANFIS Model	Inputs	MF Type (params)	Number of inputs MFs	Number of MFs	Number of Antecedent parameters	Total rules	Consequent parameters	Total parameters
AGa	4	Gaussian	2	8	16	16	80	96
AGb	4	Generalized bell	2	8	24	16	80	104
ATr	4	Trapezoidal	2	8	32	16	80	112

Volume 11, Issue 1, June 2025 - ISSN 2356-8569
http://dx.doi.org/10.21622/RESD.2025.11.1.1264

Instead of employing the conventional hybrid ANFIS training algorithm, which integrates backpropagation and the least squares error method, the proposed hybrid EPA model utilizes PSO to optimize the fuzzy inference system (FIS). The EPA model is trained to forecast these IMF components. During PSO optimization, after defining the training dataset, the FIS is generated using fuzzy c-means (FCM) clustering [43] to reduce the number of decision variables. During the training phase of the proposed model, the solar PV power generated twenty-four hours prior was decomposed using the EMD technique. Each FIS receives one component of the decomposed data along with additional meteorological inputs such as ambient temperature, diffuse radiation, and direct radiation. The solar PV power data at time instant *t* is used as the target output for training to evaluate the FIS performance. Subsequently, each FIS is fine-tuned using PSO to minimize a fitness function defined by error measures relative to the training output.

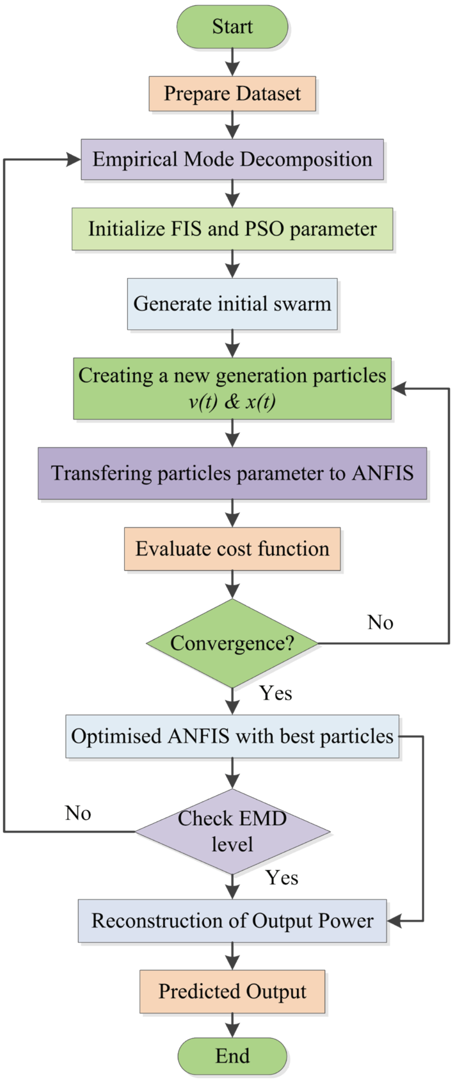

Fig. 6. EPA algorithm

As depicted in Figure 6., the EPA algorithm is implemented from start to end steps, and a detailed description of the hybrid EPA model for forecasting is provided below:

Step 1: Prepare training dataset (form matrix columns with a set of Prepossessed Solar PV power along with metrological parameters.)

Step 2: Decomposition of input

- Decompose P_s*(t-24)* using the EMD technique into IMFs and residuals.
- Define the quantity/level of IMFs.

Step3: Initialize FIS structure [44-46]

- Generate an initial fuzzy inference system for all respective intrinsic mode functions and residuals through an FCM clustering.
- Set input MF – Gaussian & output MF– linear.

Step 4: Generating the initial swarm

- Initial swarm *\$*, consisting of randomly generated *P (population size of the PSO)* particles, length of each particle's position vector *L (total number of parameters within the ANFIS)*, position of each particle p_i *(i=1,2…, P) along parameter l (l=1,2…., L) is* $\$_{p,l} = [\$_{min}, \$_{max}]$.
- Initialise $v_i^p(t)|_{t=0} = 0$ represents the initial velocity of every particle, while setting $global\_best\_\cos t = \infty$ denotes establishing the best global cost.

Step 5: Creating a new generation of particles

- The new generation of particles is formed by updating the velocity and position of the particle:

  $$v_i^{ü}(t) = \omega v_i\ (t-1) + c_1 * rand_1(P_{best} - x_i\ (t)) +$$
  $$c_2 * rand_2(G_{best} - x_i^p(t))$$
  $$x_{ü}^{ü}(t) = x\ \ (t\quad 1)\quad v\ \ (t)$$

  where v^p & x^p represent the velocity and position of the particle, respectively. The cognitive & social components are defined by the second and last terms, respectively., where c_1 and c_2 are positive acceleration constants, and *rand* generates a random number between 0 and 1.

http://dx.doi.org/10.21622/RESD.2025.11.1.1264

- The inertia weight is adjusted using the formula below:

$$\omega = \omega_{\max} - \frac{\omega_{\max} - \omega_{\min}}{I_t^{\max}} I_t$$

where $\omega_{ü}$ & $\omega_{ü}$ denote the upper and lower limits of the inertia weight, respectively. I_t represent the current iteration, while $I_t^{ü}$ signifies the maximum number of iterations.

Step 6: Transferring particle parameters to ANFIS

- Determine the dimensions of the input feature set, the count of input and output linguistic variables, and the count of elements within each linguistic variable.

- With the dimensions & count defined, the parameters of the particles are sequentially transferred to the input & output linguistic variables of the ANFIS.

Step 7: Evaluate the cost function for all particles.

- For Personal best (P_{best}) update: if the fitness value of the current position $f(x_i^p)$ of particle 'i' is better than its personal best $f(p_i)$, update the personal best position to the current position.

  If $f(x_i^p) < f(p_i)$ then $p_i = x_i^p$,
  where x_i^p is the current position of particle' i'.

- For Global best (G_{best}) update: update the global position 'g' as the position that minimises the fitness function among all the particle's personal best positions.

  $g = argmin\{f(p_1), f(p_2), \ldots\ldots\ldots, f(p_N)\}$,
  where *N* is the total number of particles in the swarm.

Step 8: Convergence criteria

- After evaluating the cost function, check that the termination criteria (max set value of iterations) are met.

- If the algorithm completes the max value of iterations, it proceeds to Step 9; otherwise, it loops back to Step 5.

Step 9: Extraction of the training process

- Extract the ANFIS output using the optimized parameters obtained through PSO.

- Finally, the training process concludes with extracting the final optimized model.

Steps 3 to 9 are repeated for each intrinsic mode function (IMF) and the residual. ANFIS models are individually trained and extracted for each IMF in a similar manner. Collective predictions are generated by combining the forecasts derived from individual models through summation. To ensure the stability of the PSO algorithm, it is recommended that (C_1+C_2) be within a specific range [47]. The parameters of the PSO algorithm used to train the ANFIS structure are presented in Table III.

TABLE III. PSO PARAMETERS USED DURING FIS OPTIMIZATION IN THE EPA HYBRID METHOD

Parameter	Value
MFs	Gaussian
Swarm size	25
Maximum number of iterations	1000
Personal learning coefficient (C_1)	1
Global learning coefficient (C_2)	2
Inertia weight	1.0
Inertia weight damping ratio	0.99

In the evaluation stage, as depicted in Figure 7, generated solar PV power $P_s(t)$ is forecasted using three PSO-FIS, i.e., PSO-FIS-1, PSO-FIS-2, and PSO-FIS-3. Each PSO-FIS receives its corresponding EMD components (*IMF-1, IMF-2, and r*) along with three meteorological variables: *T(t-24), D_f(t-48), and D_r(t-1),* as discussed in Sub-section 4.1. Level-2 IMFs are used in the empirical mode decomposition process. Instantaneous values of decomposed components $P_s^{ü\ 1}(t-24)$, $P_s^{ü\ 2}(t-24)$, $P_s^{r}(t-24)$, and their respective time instants are fed into the corresponding PSO-FIS models, along with the stated meteorological variables. The three meteorological inputs remain the same for all PSO-FISs, while the decomposed PV power data vary for each. Thus, the PSO-FIS takes the instantaneous values of the decomposed solar PV power and three meteorological features as inputs. By fine-tuning PSO parameters, the proposed hybrid model is able to generate the most favorable forecasting performance after the training phase. The PSO-FIS generates the predicted EMD-decomposed values: $P_s^{ü\ 1}(t)$, $P_s^{ü\ 2}(t)$, & $P_s^{r}(t)$. Here, the role of the ANFIS model is to learn the nonlinear

Volume 11, Issue 1, June 2025 - ISSN 2356-8569
http://dx.doi.org/10.21622/RESD.2025.11.1.1264

relationships between input features and the target output without requiring an explicit mathematical formulation, enabling accurate mapping of complex data patterns. Afterward, empirical mode reconstruction yields $P_s(t)$, the estimated solar PV power at the given time.

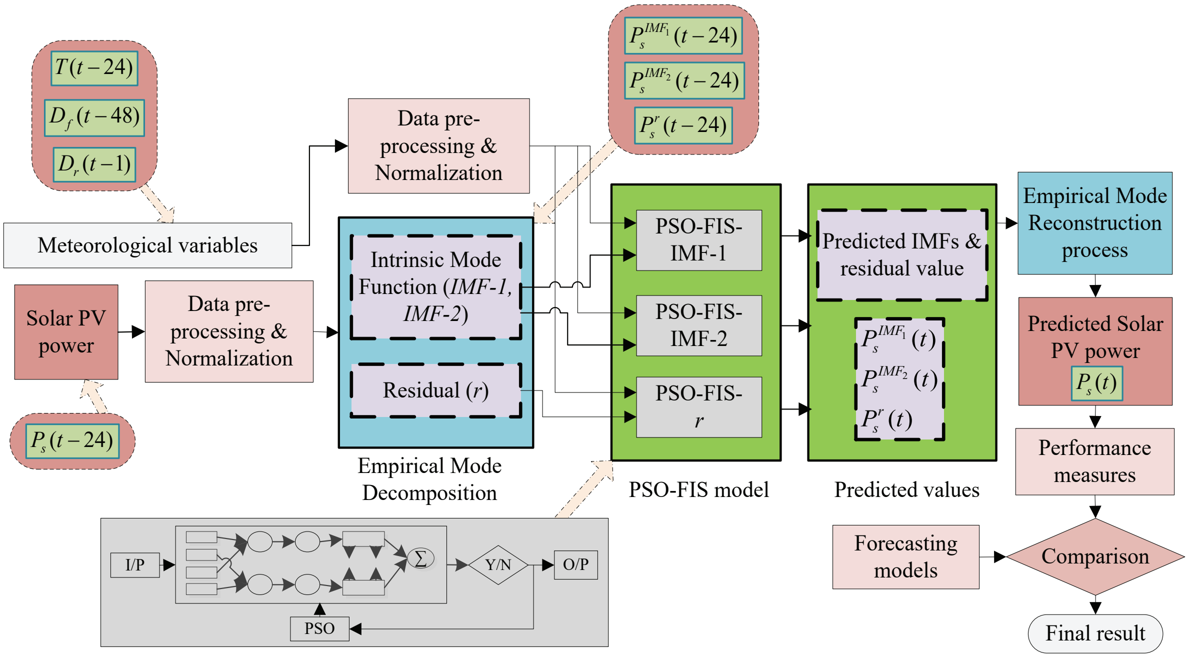

Fig. 7. Evaluation stage of the proposed hybrid EMD-PSO-ANFIS model

IV. NUMERICAL RESULT AND DISCUSSION

In this research work, the effectiveness of the hybrid EPA model is comprehensively evaluated by comparison to other forecasting models, i.e., ANN, EAGa, EAGb, and EATr-based models. A four-input hybrid EMD-ANFIS is employed with different MFs and the optimal level of IMFs and optimized using the integration of backpropagation and least squares error. In time series forecasting, it is essential to select the appropriate performance measure that will accurately assess the effectiveness of the forecasting model. Commonly used performance measures include Mean Absolute Error (MAE), Mean Square Error (MSE), and Root Mean Square Error (RMSE). These measures are often normalized to quantify the error better, as they vary linearly with the magnitude of the output parameter. Lower values of these measures indicate higher forecasting accuracy. The mathematical expressions for the MAE, MSE, RMSE, and normalized forecasting performance measures are given in (14) to (20), respectively.

$$MAE = \frac{1}{n}\sum_{v=1}^{n}|P_v - A_v| \qquad (14)$$

$$nMAE = \frac{\ddot{u}}{sd} \qquad (15)$$

$$MSE = \frac{\ }{n}\sum_{v=}^{n}(P_v - A_v) \qquad (16)$$

$$nMSE = \frac{MSE}{sd} \qquad (17)$$

$$RMSE = \sqrt{\frac{1}{n}\sum_{v=1}^{n}(P_v - A_v)^2} \qquad (18)$$

$$nRMSE = \frac{RMSE}{sd} \qquad (19)$$

$$R2 = 1 - \frac{\sum(A_v - P_v)^2}{\sum(A_v - \bar{A}_v)^2} \qquad (20)$$

Where A_v $\bar{A}_v$, and P_v, are actual power, mean of actual power, and forecasted value of v^{th} time step of any hour of the day in the dataset, respectively, sd is the standard deviation and n is the number of time stamps. All the above measures are used in this research work to evaluate the performance of various models.

http://dx.doi.org/10.21622/RESD.2025.11.1.1264

A. Training and Validation Set

A preliminary setup was assessed to determine a baseline error rate for comparison before applying optimization. Training and validation splits were used to ensure that all models were trained and evaluated on designated data partitions. Performance metrics were calculated. Table IV. shows the data sample allocation for the training, validation, and testing phases.

TABLE IV. DATA SAMPLE SPLITS FOR MODEL TRAINING AND EVALUATION

Splits	Train set (samples)	Validation set (samples)	Final test (samples)
1st Split	1 to 8181 (80%)	8182 to 9202 (10%)	-
2nd Split	-	-	9203 to 10220 (10%)

The forecasting models were validated three days ahead in two sets, for the duration of 29th-31st August and 28th-30th September. This study uses ANN and ANFIS models as benchmarks to evaluate the performance of the proposed model for solar PV power forecasting. The ANN model was developed with varying numbers of neurons in the hidden layer and trained using the Levenberg–Marquardt algorithm. RMSE and MAE were used to monitor training performance. While increasing the number of neurons led to longer training times, the improvement in forecasting accuracy was marginal. Additionally, the ANN's output varied across training runs, even with unchanged parameters. Among the tested configurations (25, 50, 80, 100, 110, and 120 neurons), the model with 80 neurons in the hidden layer provided the best balance between training time and predictive accuracy.

The ANFIS models forecast solar PV power by exploring various configurations of membership functions (MFs), including Gaussian (AGa), generalized bell (AGb), and trapezoidal (ATr), using different antecedent and consequent parameters. The performance results for these input MFs are presented in Table V.

TABLE V. PERFORMANCE OF VARIOUS ANFIS MODELS BASED ON MAE, MSE, RMSE

Date	Model	MAE	MSE	RMSE
29-31 Aug	AGa	49.52	4528	67.29
	AGb	50.23	4989	70.64
	ATr	53.33	4542	67.40
28-30 Sep	AGa	79.66	12101	110.01
	AGb	78.78	12894	113.55
	ATr	81.37	12409	111.40

From MAE, MSE, and RMSE, forecasting performance is visible in absolute format; these absolute values have their meaning when compared with models other than ANFIS. On the other hand, the forecasting performance improved when pre-processed data of ENTSOE using EMD to develop hybrid models, i.e., EAGa, EAGb, and EATr based on IMF level and MFs type. These findings are detailed in Tables VI-VIII, respectively. These results show that hybrid EAGa, EAGb, and EATr models with IMFs extracted at levels 2, 2, and 3, respectively, provide the best results. These extracted levels provided better performance than all experimented levels, i.e., level-1 to level-4. Each hybrid model is individually and rigorously investigated for its forecasting performance.

TABLE VI. PERFORMANCE MEASURES OF THE EAGa MODEL

Date	Level	MAE	RMSE	nMAE	nRMSE
29-31 Aug	1	64.55	76.55	0.0984	0.1167
	2	38.57	52.42	0.0588	0.0799
	3	44.79	52.74	0.0683	0.0804
	4	49.34	57.45	0.0752	0.0876
28-30 Sep	1	87.26	104.37	0.1291	0.1545
	2	57.26	67.77	0.0847	0.1003
	3	57.86	70.79	0.0856	0.1048
	4	59.20	71.17	0.0876	0.1053
Mean	1	75.90	90.46	0.1137	0.1356
	2	47.91	60.09	0.0715	0.0901
	3	51.32	61.76	0.0769	0.0926
	4	54.27	64.31	0.0814	0.0964

 Volume 11, Issue 1, June 2025 - ISSN 2356-8569
http://dx.doi.org/10.21622/RESD.2025.11.1.1264

TABLE VII. PERFORMANCE MEASURES OF EAGb MODEL

Date	Level	MAE	RMSE	nMAE	nRMSE
29-31 Aug	1 2 3 4	67.81 47.04 48.78 47.46	80.96 55.93 59.22 57.54	0.1034 0.0717 0.0744 0.0723	0.1234 0.0852 0.0903 0.0877
28-30 Sep	1 2 3 4	86.85 58.05 60.92 61.95	108.27 71.58 75.66 77.29	0.1285 0.0859 0.0902 0.0917	0.1602 0.1059 0.1120 0.1144
Mean	1 2 3 4	77.33 52.55 54.86 54.71	94.61 63.75 67.44 67.42	0.1159 0.0788 0.0823 0.0820	0.1418 0.0956 0.1012 0.1011

TABLE VIII. PERFORMANCE MEASURES OF THE EATr MODEL

Date	Level	MAE	RMSE	nMAE	nRMSE
29-31 Aug	1 2 3 4	76.84 47.02 45.46 45.79	90.70 58.75 55.48 57.11	0.1171 0.0717 0.0693 0.0698	0.1382 0.0895 0.0846 0.0870
28-30 Sep	1 2 3 4	73.60 55.37 52.38 56.11	96.75 64.04 61.41 65.06	0.1089 0.0819 0.0775 0.0830	0.1432 0.0948 0.0909 0.0963
Mean	1 2 3 4	75.22 51.19 48.92 50.95	93.73 61.40 58.45 61.09	0.1130 0.0768 0.0734 0.0764	0.1407 0.0921 0.0877 0.0916

From the above discussion, it is clear that hybrid EAGa, at IMF level 2, provides the best forecasting performance compared to EAGb and EATr models; therefore, for further improvement, the EAGa model is optimized using the empirical mode decomposition technique at the IMF level 2, followed by PSO with a swarm size of 25 and 1000 iterations,

TABLE IX. PERFORMANCE MEASURES OF THE EPA MODEL

Date	EMD Level	Model: EPA Forecasting Performance Measures					
		MAE	MSE	RMSE	nMAE	nMSE	nRMSE
29-31 Aug	2	32.81	1897.03	43.55	0.0500	2.89	0.0664
28-30 Sep	2	39.10	2027.33	45.03	0.0579	3.00	0.0666
Mean	2	35.96	1962.18	44.29	0.0540	2.95	0.0665

i.e., the EPA model. Among these models, EPA performs better, exhibiting mean MAE and RMSE values of 35.96 and 44.29, respectively, as depicted in Table IX. For better realization and understanding, normalized values are also tabulated in the last three columns. With this configuration, the proposed approach has superior predictive accuracy and computational efficiency compared to other models, proving its effectiveness for the given dataset and prediction framework. This analysis underscores the EPA's adaptability and reliability when properly tuned, delivering enhanced forecasting performance compared to alternative models in solar PV power estimation.

B. Final Test Set Results

The EPA hybrid model is tested with a dataset taken from a location in Greece, which includes generated solar PV power and three hourly input metrics, as earlier stated. The model demonstrates consistent hourly solar PV power forecasts over three periods: 29^{th}-31^{st} October, 28^{th}-30^{th} November, and 29^{th}-31^{st} December 2019. For a performance assessment, three advanced models, i.e., ANN, EAGa, EAGb, and EATr, are also trained and tested.

The pictorial representations of 29^{th}-31^{st} October and 29^{th}-31^{st} December 2019 are illustrated in Figs. 8 & 9., depicting the actual and forecasted solar PV power profiles obtained for ENTSOE-G. The five subplots (a)-(e) represent forecasted power trends for indicated periods. The EPA hybrid model demonstrates superior accuracy, with predicted profiles closely matching actual values, effectively capturing sudden peaks and fluctuations with minimal deviation. By considering both the external input features and historical data, EPA outperforms other approaches. As the profiles are very close to each other, a tabulation comparison is required.

http://dx.doi.org/10.21622/RESD.2025.11.1.1264

Table X. presents a comprehensive tabulation of the performance of various forecasting models. The model consistently delivers reliable hourly PV power forecasts across three periods: 29th-31st October, 28th-30th November, and 29th-31st December 2019. The proposed approach yields MAE values for these periods of 85.23, 89.86, and 84.53, respectively, and RMSE values of 105.83, 137.59, and 130.83, respectively. During the forecasted period, the EPA model exhibits exceptional performance across all mentioned periods. The EAGa model closely follows the EPA in terms of all performance measures, while the EAGb model performs notably well in December, particularly in terms of nRMSE. After observing the performance of the PSO-tuned (EPA) model, it is clear that the forecasting error obtained is the lowest among tested models. The proposed approach achieves mean nMAE, nMSE, and nRMSE values of 0.1870, 34.71, and 0.2723, respectively, over the three test periods. The proposed model shows percentage enhancements in nMAE over ANN, EAGa, EAGb, and EATr models of 24.8%, 7.97%, 13.27%, and 11.67%, respectively. Regarding nRMSE, improvements over these models are 25.6%, 6.59%, 7.66%, and 10.25%, respectively. The R-squared values for the different forecasting approaches—ANN, EAGa, EAGb, EATr, and EPA—are 0.858, 0.909, 0.908, 0.902, and 0.921, respectively. The recent analysis reveals that the EPA model achieves superior performance over a short three-day period with a one-hour lead time. Performance ranking of hybrid forecasting models in terms of nRMSE and nMAE can be seen in Figure 10 (a) and (b), respectively. Observationally, the forecasting approaches exhibit similar predicted capabilities, with their forecasted generated solar PV power profiles matching the actual data.

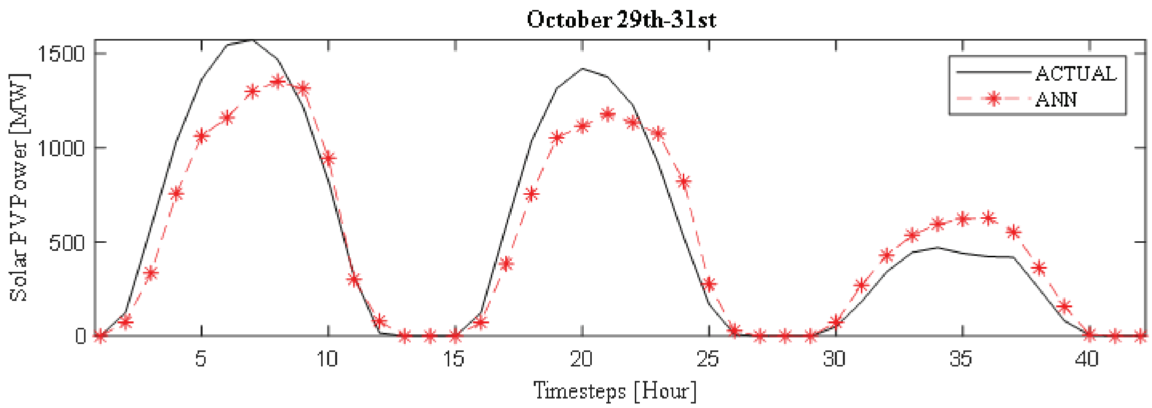

(a)

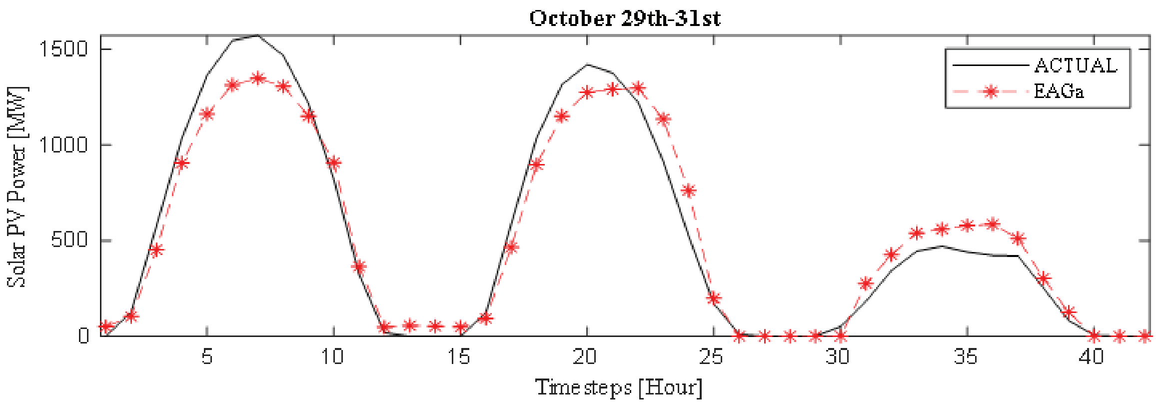

(b)

http://dx.doi.org/10.21622/RESD.2025.11.1.1264

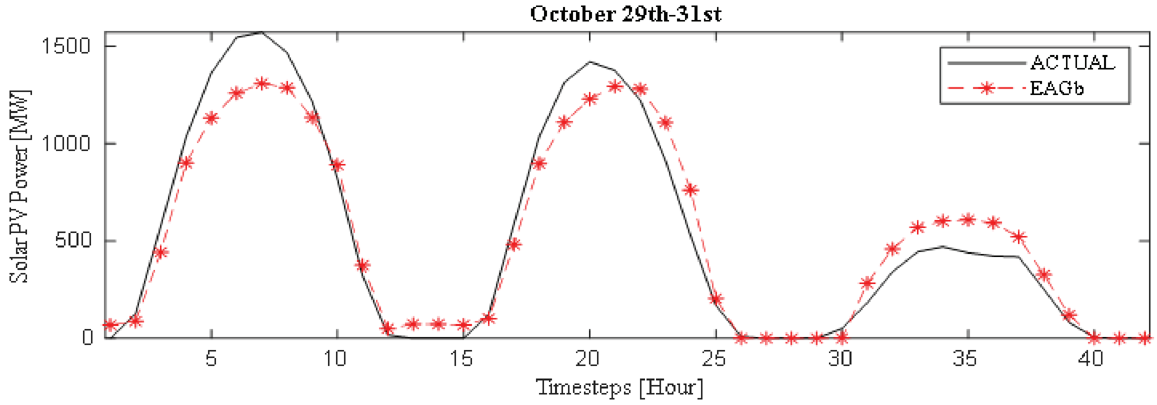

(c)

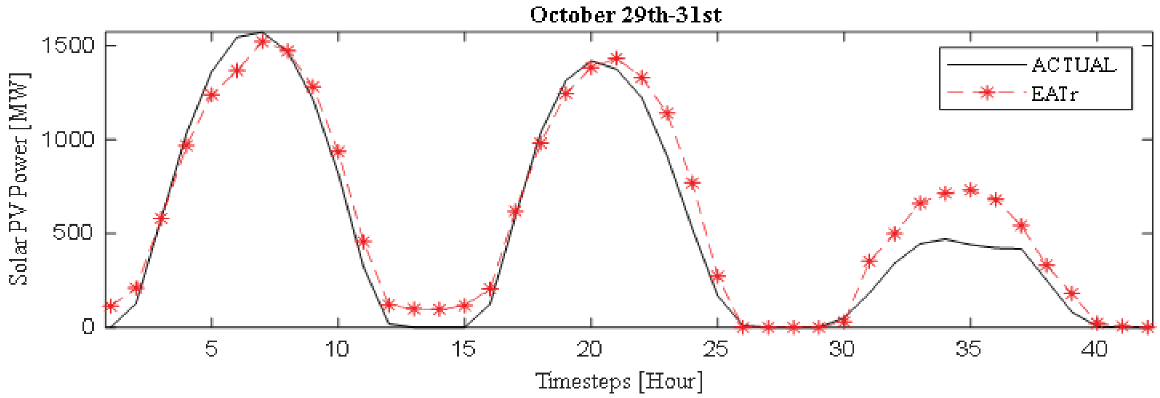

(d)

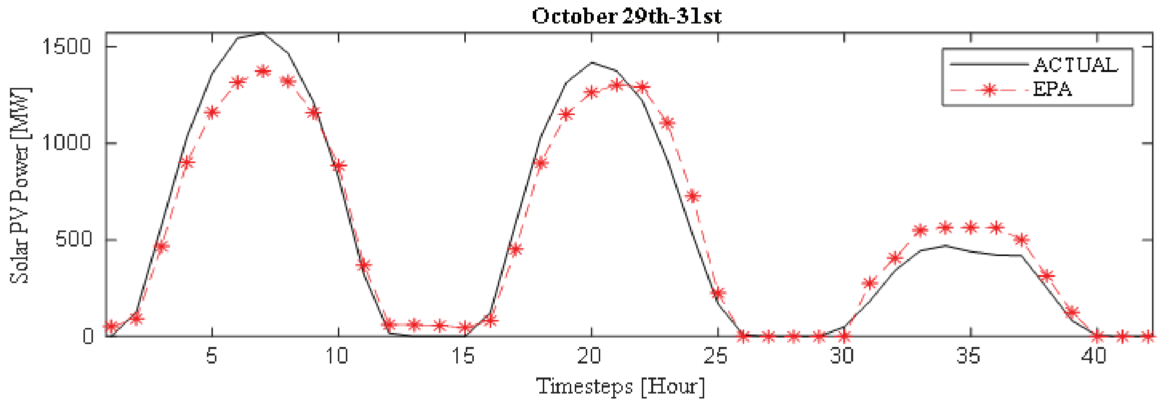

(e)

Fig. 8. Actual and forecasted solar PV power for the last three days of an October month for 42 consecutive hours (a) ANN, (b) EAGa, (c) EAGb, (d) EATr, and (e) EPA

http://dx.doi.org/10.21622/RESD.2025.11.1.1264

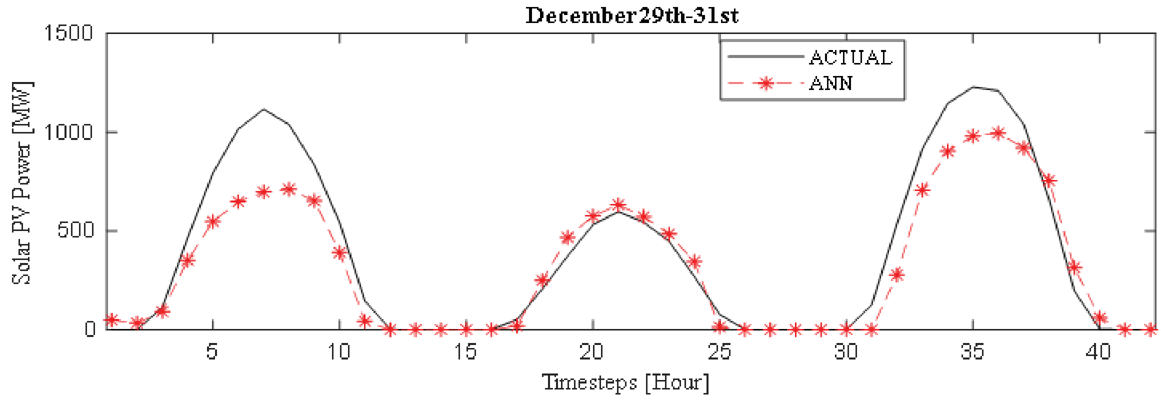

(a)

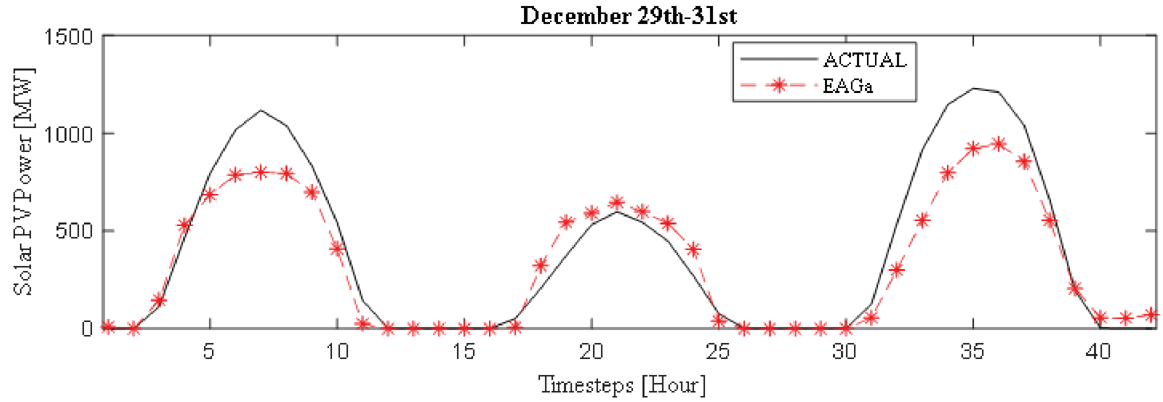

(b)

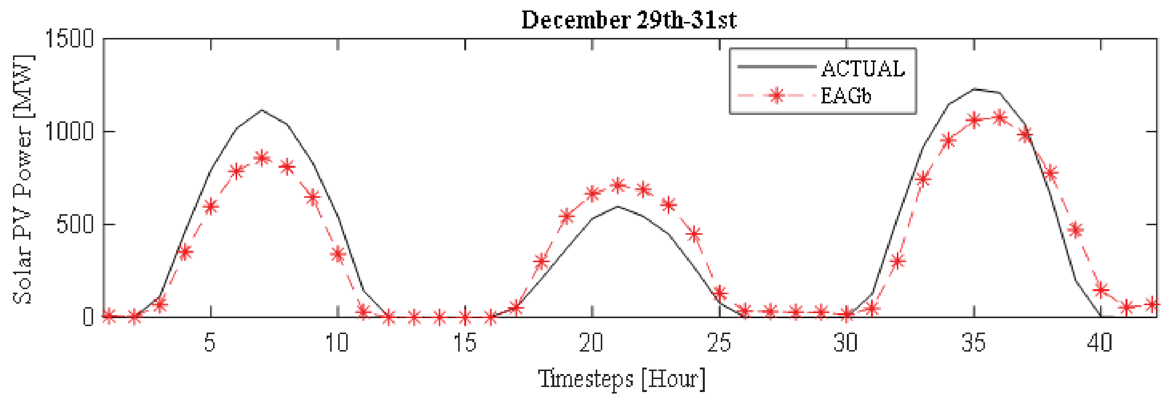

(c)

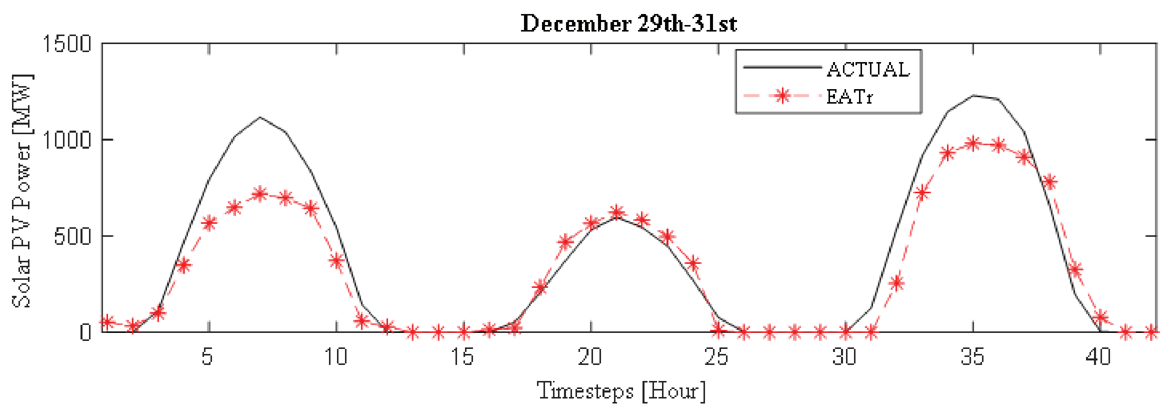

(d)

http://dx.doi.org/10.21622/RESD.2025.11.1.1264

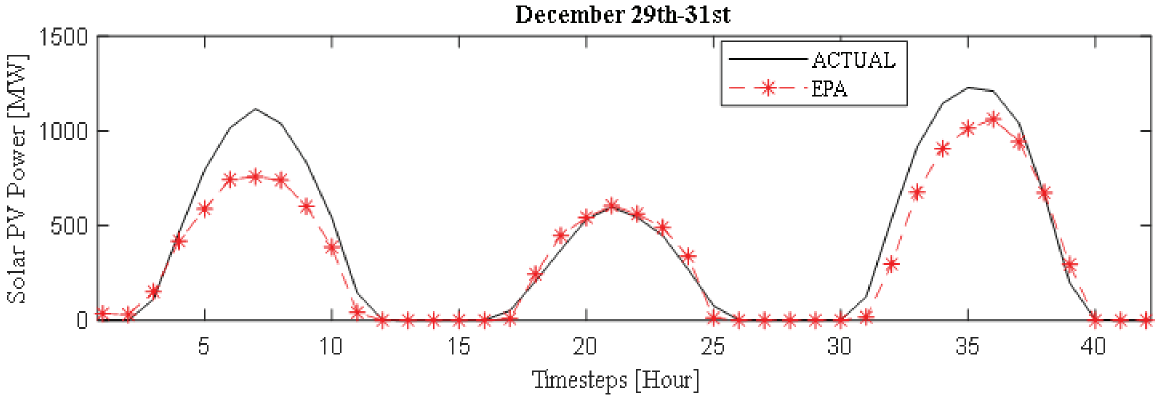

(e)

Fig. 9. Actual & forecasted solar PV power for the last three days of a December month for 42 consecutive hours (a) ANN, (b) EAGa, (c) EAGb, (d) EATr, and (e) EPA

TABLE X. EVALUATION OF DIFFERENT FORECASTING APPROACHES

Date	Performance measures	Models				
		ANN	EAGa	EAGb	EATr	EPA
29-31 Oct	MAE MSE RMSE nMAE nMSE nRMSE R2	120.16 26222 161.93 0.2217 48.38 0.2988 0.908	87.84 12505 111.83 0.1621 23.07 0.2063 0.956	98.04 15715 125.36 0.1825 28.99 0.2313 0.945	96.67 15485 124.44 0.1783 28.57 0.2296 0.946	85.23 11198 105.83 0.1572 20.66 0.1952 0.961
28-30 Nov	MAE MSE RMSE nMAE nMSE nRMSE R2	127.83 39075 197.68 0.2905 88.80 0.4492 0.793	92.22 20189 142.09 0.2096 45.88 0.3229 0.893	94.04 21815 147.70 0.2137 49.58 0.3357 0.884	95.08 20885 144.52 0.2177 47.46 0.3284 0.889	89.86 18931 137.59 0.2042 43.02 0.3127 0.899
29-31 Dec	MAE MSE RMSE nMAE nMSE nRMSE R2	99.01 21952 148.16 0.2339 51.87 0.3501 0.874	100.66 21368 146.18 0.2378 50.49 0.3454 0.877	106.09 18062 134.39 0.2507 42.68 0.3176 0.896	101.21 22216 149.05 0.2391 52.49 0.3522 0.872	84.53 17117 130.83 0.1997 40.45 0.3091 0.902
Mean	MAE MSE RMSE nMAE nMSE nRMSE R2	115.67 29083 169.26 0.2487 63.02 0.3660 0.858	93.57 18021 133.37 0.2032 39.81 0.2915 0.909	99.39 18531 135.82 0.2156 40.42 0.2949 0.908	97.89 19529 139.34 0.2117 42.84 0.3034 0.902	86.54 15749 124.75 0.1870 34.71 0.2723 0.921

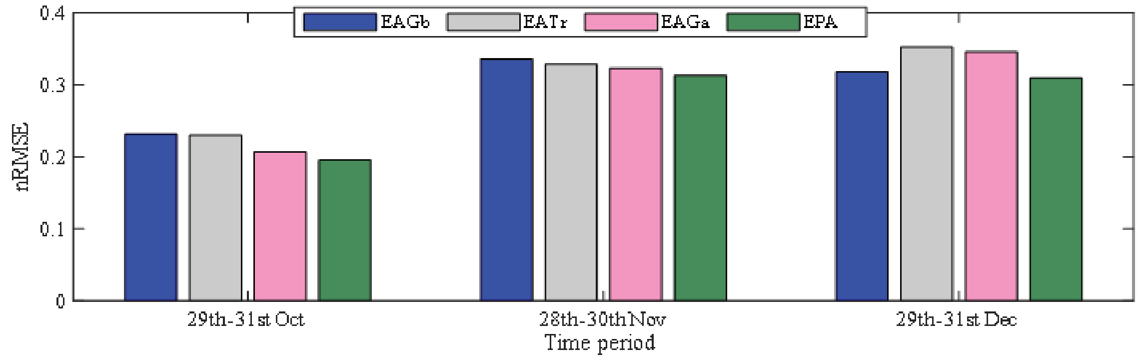

(a)

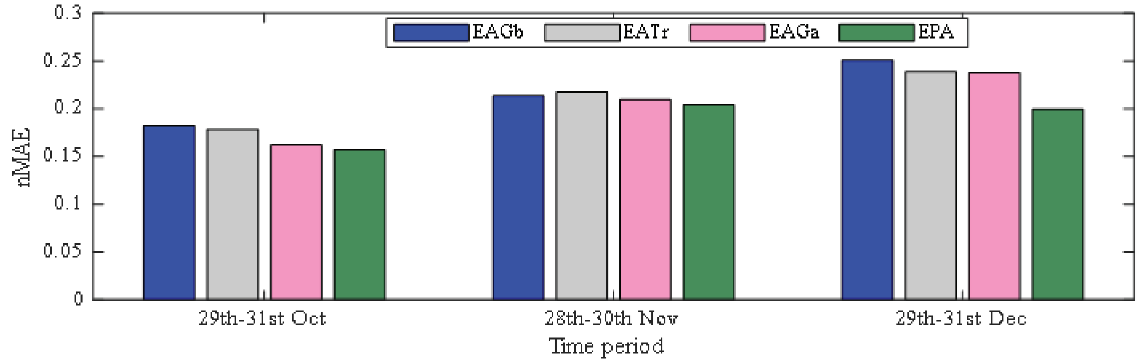

(b)

Fig. 10. Performance ranking of hybrid forecasting models in terms of (a) nRMSE and (b) nMAE

V. CONCLUSIONS

In this study, various time series forecasting models' forecast performance was analyzed, and a hybrid model— combining Empirical Mode Decomposition (EMD) with an Adaptive Neuro-Fuzzy Inference System (ANFIS) fine-tuned using PSO, referred to as EPA—was developed to forecast solar PV power in ENTSOE, Greece. Traditional forecasting approaches lack the ability to capture time-frequency signals. To address this, the proposed model decomposes the generated solar PV power into the number of Intrinsic Mode Functions (IMFs) using EMD and selects the optimal level of extracted IMFs. Various input MFs are also evaluated during FIS optimization to enhance predicting accuracy.

Comparative analyses demonstrate that the proposed hybrid EPA model outperforms other forecasting methods, achieving lower error values with an nMAE of 0.1870, nRMSE of 0.2723, and nMSE of 34.71. These results highlight the model's superior accuracy and robustness across varying meteorological conditions. Improved forecasting enables the pre-planning of operating schedules for non-renewable sources, such as thermal and nuclear plants, which require significant time to shut down and restart. Consequently, accurate forecasting and pre-planning can enhance the efficiency and reliability of overall power generation systems.

Acknowledgment:

The authors sincerely appreciate the organizers of the European Network of Transmission System Operators for Electricity, Greece (ENTSOE-G), Southeast Europe, for providing public access to solar power generation data.

Statement and declarations:

Ethics approval and consent to participate
Not applicable.

Conflict of interest
The author declares that they have no conflicts of interest.

Funding
This research has no funding or financial support from any agency.

References

[1] T. L. Kottas, Y. S. Boutalis, and A. D. Karlis, "New Maximum Power Point Tracker for PV Arrays Using Fuzzy Controller in Close Cooperation With Fuzzy Cognitive Networks," *IEEE Transactions on Energy Conversion*, vol. 21, no. 3, pp. 793–803, Sep. 2006, doi: 10.1109/TEC.2006.875430.

[2] M. Oliver and T. Jackson, "The market for solar photovoltaics," *Energy Policy*, vol. 27, no. 7, pp. 371–385, Jul. 1999, doi: 10.1016/S0301-4215(99)00038-5.

[3] U. K. Das *et al.*, "Forecasting of photovoltaic power generation and model optimization: A review," *Renewable and Sustainable Energy Reviews*, vol. 81, pp. 912–928, Jan. 2018, doi: 10.1016/j.rser.2017.08.017.

[4] M. N. Akhter, S. Mekhilef, H. Mokhlis, and N. Mohamed Shah, "Review on forecasting of photovoltaic power generation based on machine learning and metaheuristic techniques," *IET Renewable Power Generation*, vol. 13, no. 7, pp. 1009–1023, May 2019, doi: 10.1049/iet-rpg.2018.5649.

[5] M. Q. Raza, M. Nadarajah, and C. Ekanayake, "On recent advances in PV output power forecast," *Solar Energy*, vol. 136, pp. 125–144, Oct. 2016, doi: 10.1016/j.solener.2016.06.073.

[6] Y. Kashyap, A. Bansal, and A. K. Sao, "Solar radiation forecasting with multiple parameters neural networks," *Renewable and Sustainable Energy Reviews*, vol. 49, pp. 825–835, Sep. 2015, doi: 10.1016/j.rser.2015.04.077.

[7] Zhang Yun, Zhou Quan, Sun Caixin, Lei Shaolan, Liu Yuming, and Song Yang, "RBF Neural Network and ANFIS-Based Short-Term Load Forecasting Approach in Real-Time Price Environment," *IEEE Transactions on Power Systems*, vol. 23, no. 3, pp. 853–858, Aug. 2008, doi: 10.1109/TPWRS.2008.922249.

[8] J. P. S. Catalao, H. M. I. Pousinho, and V. M. F. Mendes, "Hybrid Wavelet-PSO-ANFIS Approach for Short-Term Electricity Prices Forecasting," *IEEE Transactions on Power Systems*, vol. 26, no. 1, pp. 137–144, Feb. 2011, doi: 10.1109/TPWRS.2010.2049385.

[9] M. A. Awadallah, E. H. E. Bayoumi, and H. M. Soliman, "Adaptive deadbeat controllers for brushless DC drives using PSO and ANFIS techniques," *Journal of Electrical Engineering*, vol. 60, no. 1, 2009.

[10] Nian Zhang, P. K. Behera, and C. Williams, "Solar radiation prediction based on particle swarm optimization and evolutionary algorithm using recurrent neural networks," in *2013 IEEE International Systems Conference (SysCon)*, IEEE, Apr. 2013, pp. 280–286. doi: 10.1109/SysCon.2013.6549894.

[11] C. Zhang and M. Zhang, "Wavelet-based neural network with genetic algorithm optimization for generation prediction of PV plants," *Energy Reports*, vol. 8, pp. 10976–10990, Nov. 2022, doi: 10.1016/j.egyr.2022.08.176.

[12] J. Cruz, W. Mamani, C. Romero, and F. Pineda, "Selection of Characteristics by Hybrid Method: RFE, Ridge, Lasso, and Bayesian for the Power Forecast for a Photovoltaic System," *SN Comput Sci*, vol. 2, no. 3, p. 202, May 2021, doi: 10.1007/s42979-021-00584-x.

[13] Neeraj, J. Mathew, and R. Kumar Behera, "EMD-Att-LSTM: A Data-driven Strategy Combined with Deep Learning for Short-term Load Forecasting," *Journal of Modern Power Systems and Clean Energy*, vol. 10, no. 5, pp. 1229–1240, 2022, doi: 10.35833/MPCE.2020.000626.

[14] G. Perveen, P. Anand, and A. Kumar, "Application of ANN-ANFIS Model for Forecasting Solar Power," in *Photovoltaic Systems Technology*, Wiley, 2024, pp. 151–175. doi: 10.1002/9781394167678.ch8.

[15] D. Patel, S. Patel, P. Patel, and M. Shah, "Solar radiation and solar energy estimation using ANN and Fuzzy logic concept: A comprehensive and systematic study," *Environmental Science and Pollution Research*, vol. 29, no. 22, pp. 32428–32442, May 2022, doi: 10.1007/s11356-022-19185-z.

[16] M. Viswavandya, B. Sarangi, S. Mohanty, and A. Mohanty, "Short Term Solar Energy Forecasting by Using Fuzzy Logic and ANFIS," in *Advances in Intelligent Systems and Computing*, 2020. doi: 10.1007/978-981-13-8676-3_63.

[17] E. H. M. Ndiaye, "Prediction of Photovoltaic Power Injected into the Grid Using Artificial Intelligence Algorithm: Case of Ten Merina Power Plant, Senegal," *SSRN*, 2023.

[18] A. Khosravi, S. Syri, J. J. G. Pabon, O. R. Sandoval, B. C. Caetano, and M. H. Barrientos, "Energy modeling of a solar dish/Stirling by artificial intelligence approach," *Energy Convers Manag*, vol. 199, p. 112021, Nov. 2019, doi: 10.1016/j.enconman.2019.112021.

[19] G. Didem, "Determination of industrial energy demand in Turkey using MLR, ANFIS and PSO-ANFIS," *Journal of Artificial Intelligence and Systems*, vol. 3, no. 1, pp. 16–34, 2021, doi: 10.33969/AIS.2021.31002.

[20] R. T. Moyo, M. Dewa, H. F. M. Romero, V. A. Gómez, J. I. M. Aragonés, and L. Hernández-Callejo, "An adaptive neuro-fuzzy inference scheme for defect detection and classification of solar PV cells," *Renewable Energy and Sustainable Development*, vol. 10, no. 2, p. 218, Sep. 2024, doi: 10.21622/resd.2024.10.2.929.

[21] N. Amjady, "Day-Ahead Price Forecasting of Electricity Markets by a New Fuzzy Neural Network," *IEEE Transactions on Power Systems*, vol. 21, no. 2, pp. 887–896, May 2006, doi: 10.1109/TPWRS.2006.873409.

[22] R. AbdelRassoul and Y. Ali, "A New Controller to Enhance PV System Performance Based on Neural Network," *Renewable Energy and Sustainable Development*, vol. 3, no. 2, pp. 224–233, Jun. 2017, doi: 10.21622/resd.2017.03.2.224.

[23] J. P. S. Catalao, H. M. I. Pousinho, and V. M. F. Mendes, "Hybrid Wavelet-PSO-ANFIS Approach for Short-Term Electricity Prices Forecasting," *IEEE Transactions on Power Systems*, vol. 26, no. 1, pp. 137–144, Feb. 2011, doi: 10.1109/TPWRS.2010.2049385.

[24] W. Shu and Q. Gao, "Forecasting Stock Price Based on Frequency Components by EMD and Neural Networks," *IEEE Access*, vol. 8, pp. 206388–206395, 2020, doi: 10.1109/ACCESS.2020.3037681.

[25] E. C. Loh, S. B. Ismail, and A. Khamis, "Empirical mode decomposition couple with artificial neural network for water level prediction," *Civil Engineering and Architecture*, vol. 7, no. 6, 2019, doi: 10.13189/cea.2019.071403.

[26] A. Anand and L. Suganthi, "Forecasting of Electricity Demand by Hybrid ANN-PSO Models," *International Journal of Energy Optimization and Engineering*, vol. 6, no. 4, pp. 66–83, Oct. 2017, doi: 10.4018/IJEOE.2017100105.

[27] S. Jardim, J. Valente, A. Almeida, and C. Mora, "Comparing Artificial Intelligence Classification Models to Improve an Image Comparison System with User Inputs," *SN Comput Sci*, vol. 5, no. 1, p. 57, Dec. 2023, doi: 10.1007/s42979-023-02375-y.

[28] N. E. Huang *et al.*, "The empirical mode decomposition and the Hilbert spectrum for nonlinear and non-stationary time series analysis," *Proceedings of the Royal Society of London. Series A: Mathematical, Physical and Engineering Sciences*, vol. 454, no. 1971, pp. 903–995, Mar. 1998, doi: 10.1098/rspa.1998.0193.

[29] "Data Platform", doi: https://doi.org/10.25832/time_series/2020-10-06.

[30] C. Chupong and B. Plangklang, "Forecasting power output of PV grid connected system in Thailand without using solar radiation measurement," *Energy Procedia*, vol. 9, pp. 230–237, 2011, doi: 10.1016/j.egypro.2011.09.024.

[31] C. Yang, A. A. Thatte, and L. Xie, "Multitime-Scale Data-Driven Spatio-Temporal Forecast of Photovoltaic Generation," *IEEE Trans Sustain Energy*, vol. 6, no. 1, pp. 104–112, Jan. 2015, doi: 10.1109/TSTE.2014.2359974.

[32] H. Zhu, X. Li, Q. Sun, L. Nie, J. Yao, and G. Zhao, "A Power Prediction Method for Photovoltaic Power Plant Based on Wavelet Decomposition and Artificial Neural Networks," *Energies (Basel)*, vol. 9, no. 1, p. 11, Dec. 2015, doi: 10.3390/en9010011.

[33] N. E. Huang *et al.*, "The empirical mode decomposition and the Hilbert spectrum for nonlinear and non-stationary time series analysis," *Proceedings of the Royal Society of London. Series A: Mathematical, Physical and Engineering Sciences*, vol. 454, no. 1971, pp. 903–995, Mar. 1998, doi: 10.1098/rspa.1998.0193.

[34] P. Flandrin, G. Rilling, and P. Goncalves, "Empirical Mode Decomposition as a Filter Bank," *IEEE Signal Process Lett*, vol. 11, no. 2, pp. 112–114, Feb. 2004, doi: 10.1109/LSP.2003.821662.

[35] A. Zeiler, R. Faltermeier, I. R. Keck, A. M. Tome, C. G. Puntonet, and E. W. Lang, "Empirical Mode Decomposition - an introduction," in *The 2010 International Joint Conference on Neural Networks (IJCNN)*, IEEE, Jul. 2010, pp. 1–8. doi: 10.1109/IJCNN.2010.5596829.

[36] S. Lahmiri, "Comparing variational and empirical mode decomposition in forecasting day-ahead energy prices," *IEEE Syst J*, vol. 11, no. 3, 2017, doi: 10.1109/JSYST.2015.2487339.

[37] J.-S. R. Jang, "ANFIS: adaptive-network-based fuzzy inference system," *IEEE Trans Syst Man Cybern*, vol. 23, no. 3, pp. 665–685, 1993, doi: 10.1109/21.256541.

[38] T. Takagi and M. Sugeno, "Fuzzy identification of systems and its applications to modeling and control," *IEEE Trans Syst Man Cybern*, vol. SMC-15, no. 1, pp. 116–132, Jan. 1985, doi: 10.1109/TSMC.1985.6313399.

[39] Zhang Yun, Zhou Quan, Sun Caixin, Lei Shaolan, Liu Yuming, and Song Yang, "RBF Neural Network and ANFIS-Based Short-Term Load Forecasting Approach in Real-Time Price Environment," *IEEE Transactions on Power Systems*, vol. 23, no. 3, pp. 853–858, Aug. 2008, doi: 10.1109/TPWRS.2008.922249.

[40] H.-Y. Su, T.-Y. Liu, and H.-H. Hong, "Adaptive Residual Compensation Ensemble Models for Improving Solar Energy Generation Forecasting," *IEEE Trans Sustain Energy*, vol. 11, no. 2, pp. 1103–1105, Apr. 2020, doi: 10.1109/TSTE.2019.2931154.

[41] A. Mellit and S. A. Kalogirou, "ANFIS-based modelling for photovoltaic power supply system: A case study," *Renew Energy*, vol. 36, no. 1, pp. 250–258, Jan. 2011, doi: 10.1016/j.renene.2010.06.028.

[42] I. M. El-Hasnony, S. I. Barakat, and R. R. Mostafa, "Optimized ANFIS Model Using Hybrid Metaheuristic Algorithms for Parkinson's Disease Prediction in IoT Environment," *IEEE Access*, vol. 8, pp. 119252–119270, 2020, doi: 10.1109/ACCESS.2020.3005614.

[43] Y. K. Semero, D. Zheng, and J. Zhang, "A PSO-ANFIS based Hybrid Approach for Short Term PV Power Prediction in Microgrids," *Electric Power Components and Systems*, vol. 46, no. 1, pp. 95–103, Jan. 2018, doi: 10.1080/15325008.2018.1433733.

[44] V. A. Okolobah and Z. Ismail, "A new approach to peak load forecasting based on EMD and ANFIS," *Indian J Sci Technol*, vol. 6, no. 12, 2013, doi: 10.17485/ijst/2013/v6i12.9.

[45] K. Kampouropoulos, F. Andrade, E. Sala, A. G. Espinosa, and L. Romeral, "Multiobjective Optimization of Multi-Carrier Energy System Using a Combination of ANFIS and Genetic Algorithms," *IEEE Trans Smart Grid*, vol. 9, no. 3, pp. 2276–2283, May 2018, doi: 10.1109/TSG.2016.2609740.

[46] M. Ali, M. Adnan, M. Tariq, and H. V. Poor, "Load Forecasting Through Estimated Parametrized Based Fuzzy Inference System in Smart Grids," *IEEE Transactions on Fuzzy Systems*, vol. 29, no. 1, pp. 156–165, Jan. 2021, doi: 10.1109/TFUZZ.2020.2986982.

[47] J. Kennedy, "The behavior of particles," 1998, pp. 579–589. doi: 10.1007/BFb0040809.